energies

MDPI

Article

# Maximum Power Extraction from a Partially Shaded PV System Using an Interleaved Boost Converter

**Hassan M. H. Farh [1,2,*], Mohd F. Othman [1], Ali M. Eltamaly [3,4] and M. S. Al-Saud [2,5]**

1 Malaysia-Japan International Institute of Technology, Universiti Teknologi Malaysia, Kuala Lumpur 54100, Malaysia; mdfauzi@utm.my
2 Electrical Engineering Department, College of Engineering, King Saud University, P.O. Box 800, Riyadh 11421, Saudi Arabia; mamdooh@ksu.edu.sa
3 Electrical Engineering Department, Mansoura University, Mansoura 35516, Egypt; eltamaly@ksu.edu.sa
4 Sustainable Energy Technologies Center, King Saud University, P.O. Box 800, Riyadh 11421, Saudi Arabia
5 Saudi Electricity Company Chair in Power System Reliability and Security, King Saud University, Riyadh 11421, Saudi Arabia
* Correspondence: mahhhassan2@graduate.utm.my or hfarh1@ksu.edu.sa; Tel.: +966-50-050-7630

Received: 23 July 2018; Accepted: 17 September 2018; Published: 24 September 2018


**Abstract:** The partially shaded photovoltaic (PSPV) condition reduces the generated power and contributes to hot spot problems that may lead to breakdown of shaded modules. PSPV generates multiple peak, one global one and many other local peaks. Many efficient, accurate and reliable maximum power point tracker (MPPT) techniques are used to track the global peak instead of local peaks. The proposed technique is not limited to global peak tracking, but rather it is capable of tracking the sum of all peaks of the PV arrays using an interleaved boost converter (IBC). The proposed converter has been compared with the state of the art conventional control method that uses a conventional boost converter (CBC). The converters used in the two PSPV systems are interfaced with electric utility using a three-phase inverter. The simulation findings prove superiority of the PSPV with IBC compared to the one using CBC in terms of power quality, reliability, mismatch power loss, DC-link voltage stability, efficiency and flexibility. Also, IBC alleviates partial shading effects and extracts higher power compared to the one using CBC. The results have shown a remarkable increase in output generated power of a PSPV system for the three presented scenarios of partial shading by 61.6%, 30.3% and 13%, respectively, when CBC is replaced by IBC.

**Keywords:** partially shaded photovoltaic; conventional boost converter; interleaved boost converter; maximum power point tracker; utility grid; mismatch loss

## 1. Introduction

Solar photovoltaic (PV) energy systems are considered as some of the most promising options of the renewable generation systems (RGSs) which are clean, abundant, noise free and friendly to the environment compared to the conventional energy resources such as natural gas, fossil fuel, coal, etc. For these reasons, RGSs, especially solar and wind, are attracting interest all over the world. In addition, tracking the maximum power from these RGSs and choosing a suitable power electronics converter that matches the utility grid requirements are considered to be a hot development area as it can improve the system's efficiency, reliability, power quality and flexibility [1–4].

Partial shading (PS) occurs when some cells or modules of a PV system are partially or totally shaded due to aging, damage, dust, moving clouds during the day or neighboring buildings and towers. Some reasons may appear with time and cause PS after the installation of the PV energy system. The shaded PV modules have a negative effect on the generated output power and overall

efficiency of the PV system. Furthermore, hot-spot and thermal breakdown problems may occur, where the protection of the PV modules using bypass diodes is inevitable [5–8]. Under partial shading conditions (PSCs), the P-V characteristic contains one global peak (GP) and many local peaks (LPs) instead of the unique peak under uniform conditions as shown in the P-V characteristic of Figure 1. Conventional MPPT techniques such as Hill Climbing (HC), Perturb and Observe (P&O), and Incremental Conductance (IC) [9–15] are quite simple to implement and acceptable in tracking the unique MPP under uniform conditions. However, they are not efficient in tracking the GP under PSCs as they do not have the ability and intelligence to distinguish between LPs and GP. Additionally, solar irradiance with rapid fluctuations can cause these MPPT techniques to track the MPP direction inaccurately [16–20]. The power losses of the PV system due to PSCs or inaccurate GP tracking is extraordinarily high, and may exceed 70% of the total generated power. Consequently, tracking the GP is of interest in order to achieve high power efficiency, less power losses, and high output power [21].

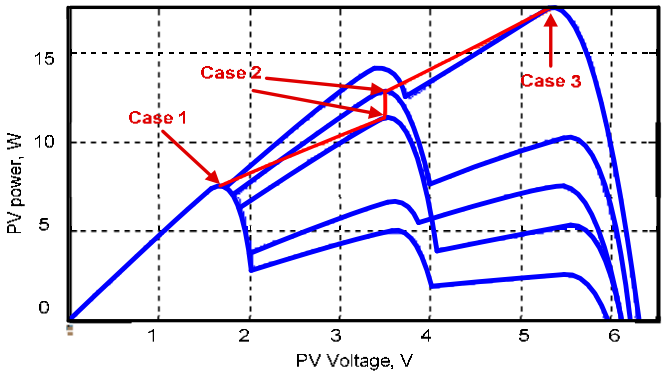


**Figure 1.** P-V characteristics of partially shaded photovoltaic (PSPV) arrays.

In recent years, many studies have been carried out to track the GP instead of LPs using efficient soft computing techniques to improve the maximum power extracted and overall efficiency [22–32]. These techniques differ in terms of simplicity, cost, design, performance, tracking speed, efficiency, robustness and accuracy. In addition, each technique has its own merits and demerits. For example, Titri et al. proposed a new bio-inspired (BI) technique called ant colony optimization based on a new pheromone update (ACO_NPU) to track the GP under PSC [22]. The obtained ACO_NPU MPPT was analyzed, investigated and compared to conventional the P&O MPPT technique and MPPT artificial intelligence (AI)-based techniques such as artificial neural network (ANN), fuzzy logic controller (FLC), artificial neural fuzzy interface (ANFIS) and fuzzy logic genetic algorithm (FL-GA) MPPT techniques. It was also compared with the BI particle swarm optimization (PSO) and ACO. The results showed superior performance of BI methods like ACO, and PSO in terms of convergence speed, accuracy, stability and robustness [22]. On the other hand, an improved PSO technique, IPSO [23–25] is used for tracking the GP accurately and almost without oscillation due to the cooperation and competition between particles. It updates the particle's speed and position continuously to track the GP through sending the optimal duty cycle to the DC-DC converter [23,26–29]. Finally, the researchers in [30–33] proved the effectiveness of the AI techniques such as ANN, FLC, genetic algorithm (GA) and hybrid techniques (e.g., neuro-fuzzy or ANFIS and FL optimized by GA) in terms of accuracy, quick response, flexibility, power consumption and implementation simplicity. In spite of the capability of these modern MPPT techniques to track the GP, it is still lower than the sum of all individual peaks of the PSPV system. An interleaved boost converter (IBC) interfaced with multi-PV arrays is one of the most effective solutions to mitigate PS effects and enhance the ability to extract the maximum power available from the whole PSPV system, which are newly introduced in this paper. Using IBC, the whole PV system performance is improved in terms of power quality, reliability, DC-link voltage stability and overall efficiency. It can be used for high voltage, high current, and high power applications in different industrial purposes. In addition, IBC has many attractive features such as: (i) minimal input

current ripples; (ii) boosting the output voltage to higher levels; (iii) reducing the thermal stresses on the devices; (iv) lower current stress on the power switches and inductance hence; reducing the passive components size; (v) higher output power and efficiency; and (vi) higher power density [34–39].

In one of the earliest works on interleaved DC-DC converters they were used over 40 years ago to design a power supply for the Jet Propulsion Laboratory [40]. Benyahia et al. investigated the P&O MPPT performance with IBC for fuel cell generators supplying electricity to a power train [41]. In another study, Arango et al. proposed asymmetrical interleaved DC-DC converters and a voltage multiplier cells combined together (boost, buck-boost and flyback-based) for PV and fuel cell applications to achieve high output voltage and ripple reduction in the generator and load [42]. However, variable DC-link voltage was generated and two DC-DC converters were used for each PV array that resulted in total cost increase. A study by Deihimi et al. also investigated the performance of variable IBC (series-connected) but it interfaced with multi energy sources of different outputs [43]. Although variable IBC provides higher voltage gains in addition to a wide range of applications from low to high voltage/power, the DC-link voltage is unstable (variable) [44]. Hence, the whole system will operate in asymmetric condition and the maximum power generated from PSPV cannot be captured. Therefore, variable IBC is not able to mitigate and fix the DC-link voltage variations. As a result, it is not preferred to be applied with the PSPV system where the irradiance of all PV modules/strings/arrays is different, and the output voltage/current of each DC-DC converter is not the same. Hence, fixed IBC is the best choice to enhance the stability of DC-link voltage. Recently, many literature studies [45–55] have been done to prove the superiority of the interleaved DC-DC converters compared to the CBC with constant input power in terms of ripples, energy savings, efficiency, steady state, electromagnetic emission, and reliability. For example, the researchers in [47,50,52] have shown the possibility of using IBC with PV in terms of reliability evaluation, ripple reduction and faster transient response. However, they performed their studies on standalone PV without PS in order to highlight the IBC performance where the input power is constant, which is different under PSCs. On the other hand, the researchers in [43,45,46,48,53] demonstrated the possibility of using IBC for high voltage applications compared to the CBC, whereas, Rehman et al. introduced a detailed comparisons of interleaved DC-DC converter topologies in terms of cost, reliability, flexibility and efficiency that can be used in renewable energy applications [54]. The latter proved that buck and boost are more reliable, less cost and more efficient while Cuk and single-ended primary-inductor converter (SEPIC) converters are more flexible than others as they are ripple free and able to increase or decrease the output voltage. Finally, Ngai-Man et al. proved the better performance of a two-phase IBC using the SiC diodes compared to IBC using the Si diodes in addition to high efficiency and high power density [55]. This is supported by the study of Mouli et al. which revealed that higher power density was obtained with SiC IBC (2.5 times) compared to the Si IBC interfaced with the 10-kW PV for tracking the MPP [56].

On the basis of this comprehensive literature review, the study shown in this paper may be counted as the first study to show the improvement of PSPV system performance in case of PSC using IBC. It is an effective and efficient solution, not only to remedy the PS effects but also to extract the summation of individual maximum power available from each PV array branches which is greater than the GP tracked from the PSPV system with CBC. The performance of IBC interfaced with multi partially shaded photovoltaic (PSPV) arrays interconnected to the utility grid—which has never been done before—will be analyzed and investigated in this paper. To achieve this purpose, performance comparisons between the proposed PSPV system with IBC and another PSPV system with CBC have been carried out and investigated in terms of power quality, reliability, mismatch power loss and overall efficiency. Also, future enlargements of the PV system can be easily adopted where multi-PV arrays can be added easily as an add-on option with their own boost converter into the existing PV system. Finally, the adequacy of whether the variable or fixed interleaved DC-DC converter is adequate or not to PSPV grid connected will be investigated. As a result, the best IBC topology to achieve the DC-link voltage regulation and extract the maximum power available from the whole PSPV system

interfaced with the utility grid is determined and presented. The findings of this study can open the door for the PV designers and researchers to adopt IBC that interfaced with the PSPV system to maximize the output power generated.

## 2. Description of the PSPV Systems with and without IBC

### *2.1. Grid-Connected PSPV Energy System with CBC*

Figure 2 shows a PV energy conversion system, where the PV array is connected to the utility grid through CBC and three-phase inverter. Inputs to the PV array are Sun irradiance ($W/m^2$) and cell temperature (°C). Three PV arrays WITH three different radiations are used to represent the PSCs. As a consequence of PSCs, multiple peaks are generated; three peaks; and the occurrence of the GP is at different places of the P-V curve. Three different shading patterns with three different cases (Case 1; GP at the beginning, Case 2; GP at the middle, Case 3; GP at the end) are used successively. The first shading pattern (GP at the beginning) is followed by the second shading pattern (GP at the middle) which is followed by the last shading pattern (GP at the end) as shown in Figure 3. Each PV array contains 54 parallel strings and 5 series modules per string with a peak power of 50 kW; hence the maximum power available from the whole PV energy system is 150 kW. In this PSPV system, the improved or deterministic PSO (DPSO) is used as an efficient GP tracker to track the GP power. This goal has been achieved via searching the optimal duty cycle of the CBC that extracts the GP as shown in Figure 3. Nevertheless, tracking the GP power does not mean that the maximum power available from the PSPV system has been achieved. The GP power is always less than the summation of maximum power available from the individual arrays of PSPV energy system which will be discussed in the simulation results section. The mismatch loss index, *MML* which determines the relation between the maximum power of the whole system and the sum of all peaks can give an indication about the power quality. It can be calculated mathematically as follows [7]:

$$MML = \frac{\text{Maximum Power of the whole system}}{\sum_{1}^{N} P_{\max}(i)} \quad (1)$$

where, $i$ is the index for PV modules and $N$ is the total number of PV modules/arrays.

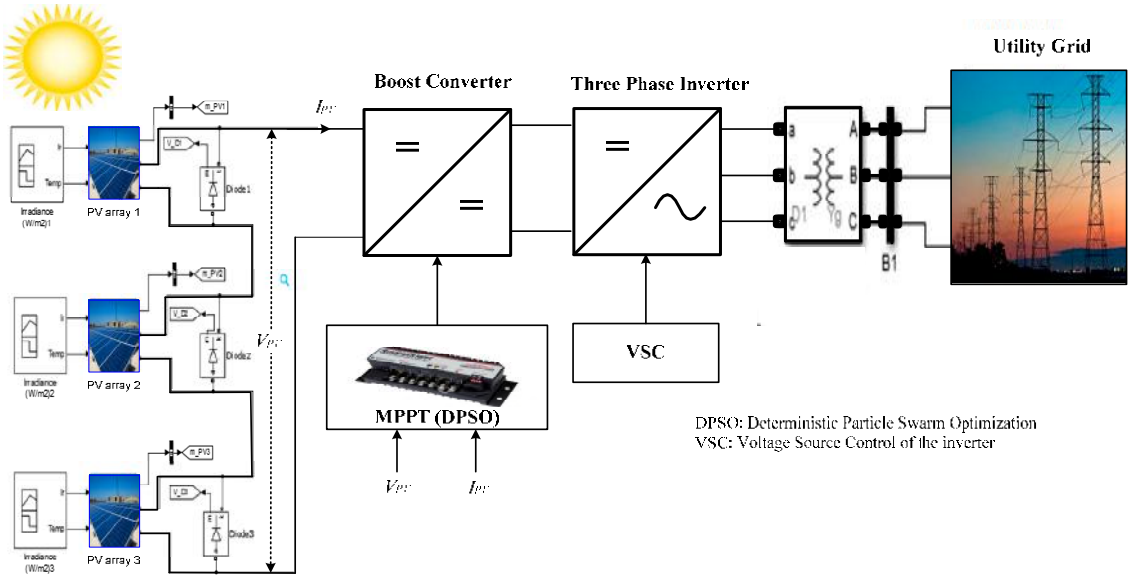


**Figure 2.** Multi-PV grid-connected system with conventional boost converter (CBC).

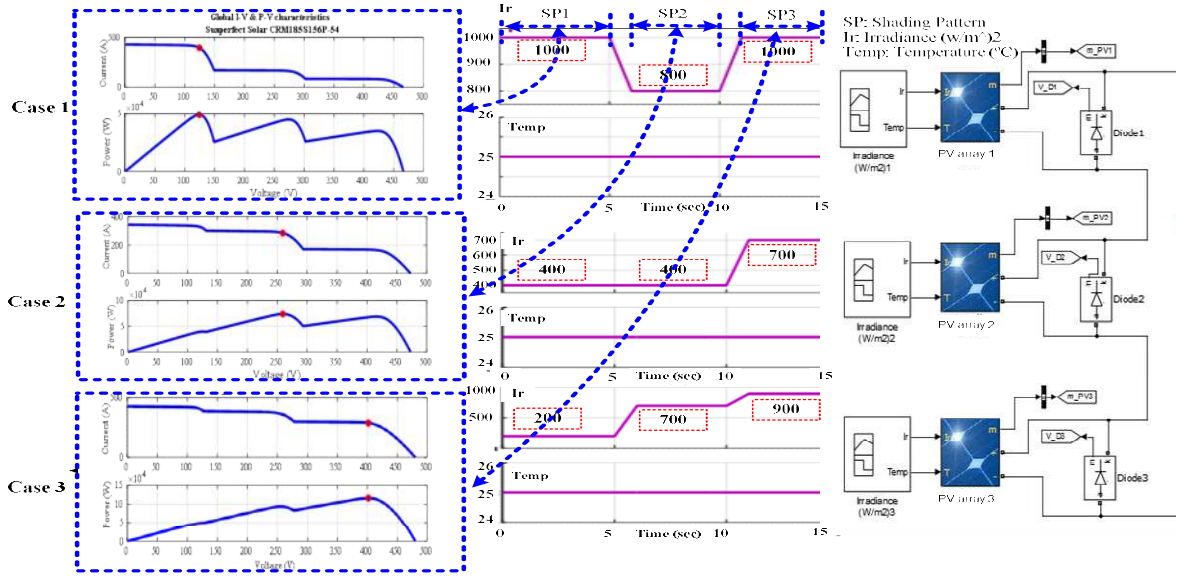


**Figure 3.** Three different partial shading cases of the PV arrays under study.

## 2.2. Grid-Connected PSPV Energy System with IBC

Multi-PV arrays which are interconnected to the utility grid through IBC and pulse width modulation voltage source converter (PWM-VSC) are shown in Figure 4. The idea behind using IBC interfaced with multi-PV arrays is to reduce the ripple current, improve the power quality, regulate the DC-link voltage, and enable the use of independent MPPT control of each PV array to achieve higher output generated power and increase the overall efficiency. Also, this proposed PV system remedies and alleviates the PS effects related to the maximum power of the system and its efficiency. Each PV array works at its own MPP that is being tracked by a separate MPP tracker through providing the duty cycle to its own boost converter. Different duty cycles are provided for each branch of the IBC where a separate MPP tracker P&O is used for each PV array to track its unique MPP as shown in Figure 4. Hence, the proposed multi-PV with IBC works at its MPP and the total maximum power delivered by this PSPV system is the summation of all peaks which is greater than the GP tracked from the previous PSPV system with CBC as will be shown later in the simulation results section.

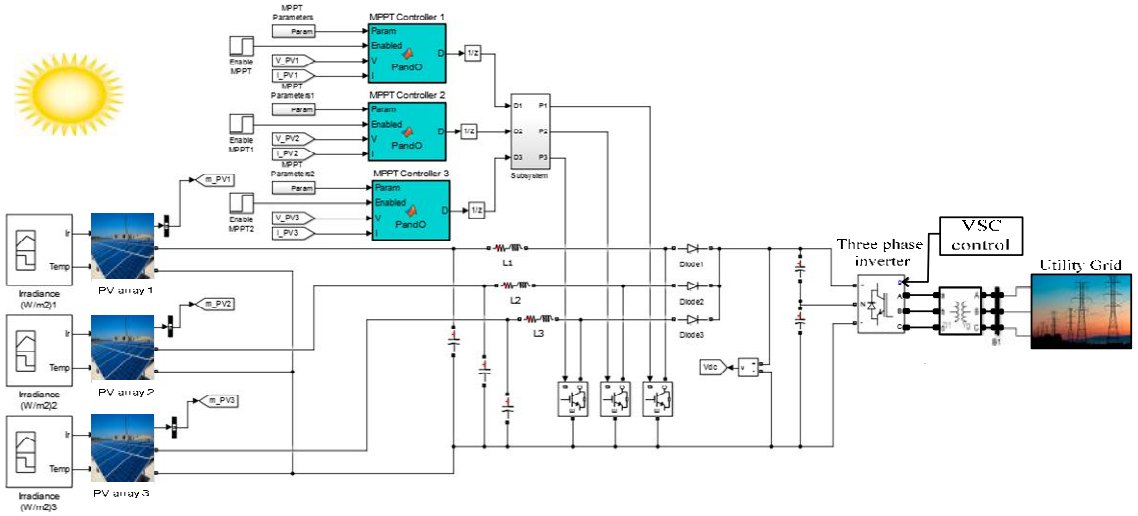


**Figure 4.** Multi-PV arrays with interleaved boost converter (IBC) interfaced the utility grid.

The simulations of the two PSPV energy systems with and without IBC are carried out using MATLAB/Simulink (ver2016, MathWorks, Natick, MA, USA). The same three PV-arrays with the same characteristics and inputs (Irradiance and temperature) of the previous PSPV system with CBC are used here to investigate, analyze and compare the response and performance of the two proposed PV systems. The purpose of these comparisons and analysis is to determine the best choice of a boost converter to deal with the PS in terms of output power generated, power quality, DC-link voltage stability and participation of PS mitigation. The inverter active and reactive power output can be controlled according to the following equations [57]:

$$P_{out} = \frac{\sqrt{3}\, m_a\, V_{dc}\, V_{sys}}{2\sqrt{2}X_T} \sin(\delta) \tag{2}$$

$$Q_{out} = \frac{\sqrt{3}\, V_{dc} V_{sys}}{2\sqrt{2}X_T} \cos(\delta) - \frac{(V_{sys})^2}{X_T} \tag{3}$$

where; $V_{sys}$ is the utility voltage, $X_T$ is the reactance between the inverter and utility system, $V_{dc}$ is the DC-link voltage and $\delta$ is the inverter voltage angle.

## 3. Maximum Power Point Tracking under Partial Shading Conditions

### *3.1. Particle Swarm Optimization Technique*

The particle swarm optimization (PSO) technique represents one of the most efficient BI techniques. It can track the GP accurately with low oscillation. The GP tracking depends on the particle's velocity and position which are renewed and updated to track the GP instead of LPs by sending the duty cycle to the boost converter [22–25]. Each particle in the swarm has mainly two variables; the position vector ${x_i}^k$ and the velocity vector ${v_i}^k$ and the new position can be calculated as follows [23]:

$${x_i}^{k+1} = {x_i}^k + {v_i}^{k+1} \tag{4}$$

The new position of the particle is determined through calculating the velocity using current position ${x_i}^k$, particle velocity ${v_i}^k$, and global best position $G_{best}$ as follows:

$${v_i}^{k+1} = \omega {v_i}^k + c_1 r_1 \left(P_{best\ i} - {x_i}^k\right) + c_2 r_2 \left(G_{best} - {x_i}^k\right) \tag{5}$$

where, $\omega$ is the inertia weight that determines the research area. It can be set to constant value (0.5) or variable to accelerate the GP tracking [24]. $c_1$ and $c_2$ are the acceleration coefficients where, $c_1$ is self-confidence and $c_2$ is swarm-confidence. The range of $c_1$ varies from 1.5 to 2 while the range of $c_2$ varies from 2 to 2.5 [58]. Authors in [23] used the duty cycles of the DC-DC converter as the positions of the PSO particles. The PSO algorithm begins the search by sending initial duty cycles to the DC-DC converter and the obtained PV voltage and current are used to compute the $P_{best}$ and $G_{best}$ values as shown in the PSO flowchart in Figure 5. The new duty cycles are computed using the velocity and position equations, based on Equations (4) and (5).

Some authors [27–29,59,60] used the conventional PSO which is able to handle PSCs and track the GP accurately, but they discovered that it is low during the steady state oscillations [24]. As a result, others in [25,61] have added some modifications to it. Later an improved or a deterministic PSO (DPSO) was proposed to improve the tracking capability of the conventional PSO, where the random number in the velocity equation is removed as follows [25]:

$${v_i}^{k+1} = \omega {v_i}^k + \left(P_{best\ i} - {x_i}^k\right) + \left(G_{best} - {x_i}^k\right) \tag{6}$$

$${v_i}^{k+1} = \omega {v_i}^k + \left(P_{best\ i} + G_{best} - 2{x_i}^k\right) \tag{7}$$

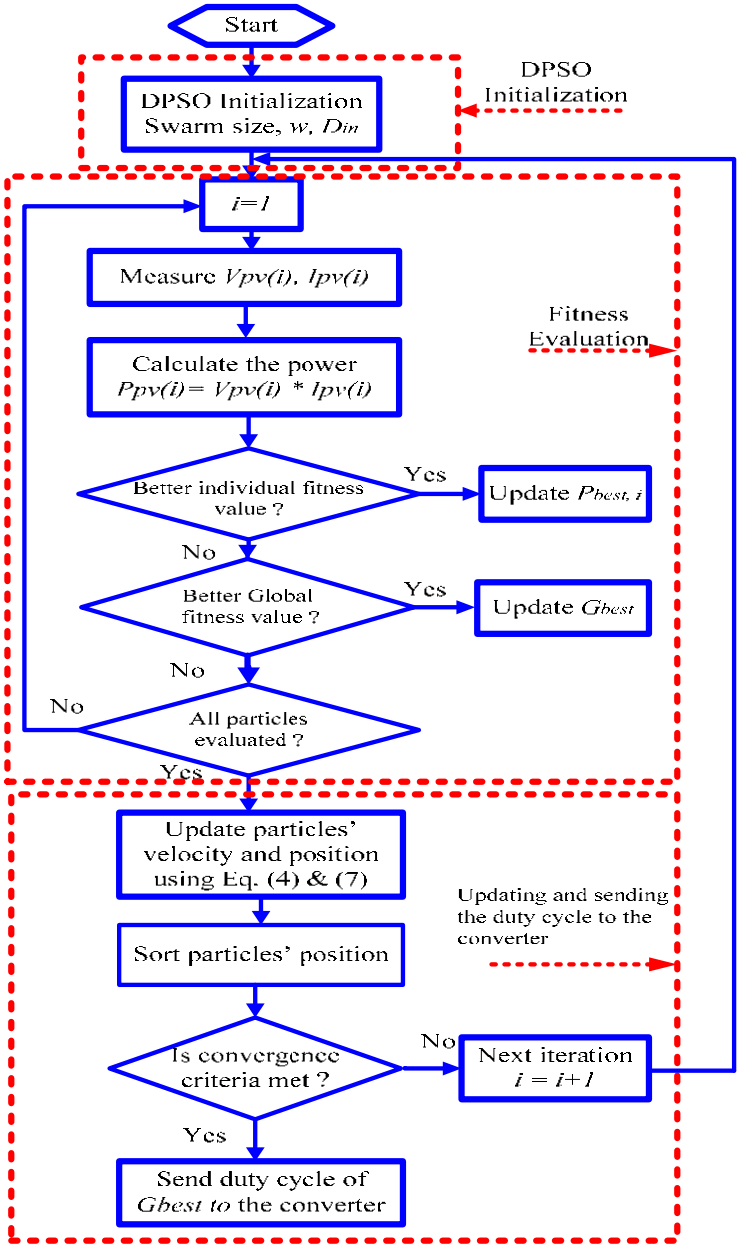


**Figure 5.** The Flowchart of deterministic particle swarm optimization (DPSO) based maximum power point tracker (MPPT).

The DPSO has many advantages compared to the conventional PSO such as simple structure, more satisfactory performance and furthermore a consistent solution can be achieved for smaller number of particles. Also, only one parameter needs to be tuned (the inertia weight). Additionally, the DPSO has faster tracking speed, robust, and almost zero steady-state oscillation compared to HC or any other MPPT techniques [25]. On the other hand, Soltani et al. proved the superiority performance of conventional PSO, IPSO, quantum inspired PSO, QPSO, vector evaluated PSO, VEPSO and PSO with time varying acceleration coefficients, PSOTVAC techniques in terms of fast response and high accuracy compared to the conventional P&O technique. Also, conventional PSO has the fastest response among all PSO techniques and PSOTVAC is more accurate in tracking the GP than others [61]. According to the literature [23,25,26,28,29,62–64], the results proved the significant performance of the BI techniques especially PSO, cuckoo search optimization (CSO), Modified firefly (MFA) and ACO to track the GP in all cases of PS in terms of convergence speed, accuracy, stability and robustness. As a result, the

maximum power extraction from the grid-connected PSPV energy system with CBC is carried out using DPSO technique. The DPSO logic steps used in the simulation is summarized as follows:

- Step 1 (DPSO initialization): Send the initial duty cycles to CBC of the PSPV system one by one and collect the related power values.
- Step 2 (Updating the velocity and position of particles): Update the position and velocity for each particle using Equations (4), and (7), respectively, and consequently get the new values of duty cycles.
- Step 3 (Fitness evaluation): Send the new values of duty cycles to the PSPV system and collect the related power values.
- Step 4 Evaluate the $P_{best,i}$, $G_{best}$ and their associated particle's position (duty cycles), then; go back to Step 2.

### 3.2. Perturb and Observe Technique

The maximum power from the grid-connected PSPV energy system with IBC can be tracked easily and efficiently using P&O technique. As shown previously in Figure 4, independent MPP tracker is used for each PV array to track its unique MPP. Multi-PV arrays interfaced with IBC does not only alleviate and mitigate the negative effects of PS but also guarantees that each PV array branch works at its own MPP and the total maximum power extracted from this system is the sum of all peaks of individual arrays. Tracking the maximum power from the multi-PV arrays is achieved through controlling the duty cycles of the IBC separately where three different duty cycles are sent from the three MPP trackers.

The P&O based MPPT uses the operating voltage perturbation of the array and observes the output power variation. If the power increased with the last voltage increment, then the next perturbation must be kept in the same direction as shown in Figure 6. On the other hand, if the voltage increment reduces the power, the next perturbation must be reversed. The maximum power is achieved when $d_P/d_V = 0$ [65,66]. Figure 7 shows the flow chart of P&O technique.

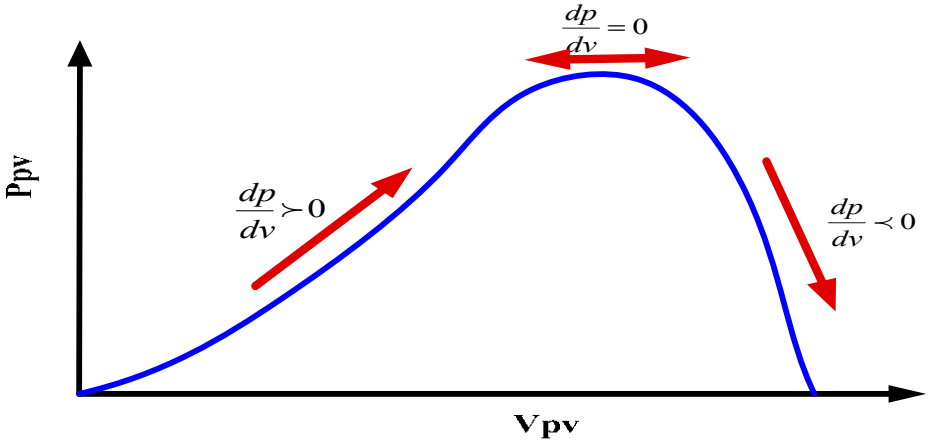


**Figure 6.** P-V characteristic of the PV array.

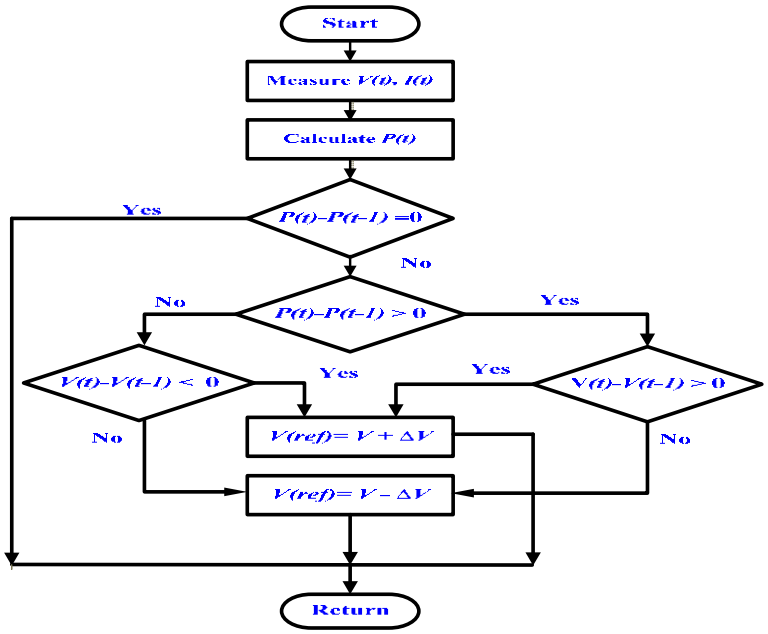


**Figure 7.** The flow chart of Perturb and Observe (P&O) technique.

## 4. Simulation Results and Discussion

The two different grid-connected PSPV systems are simulated in MATLAB/Simulink (V2016). The first PV system consists of three PSPV arrays having the same characteristics with a total maximum power of 150 kW. Three different shading patterns are selected to cover all possible PSC cases (GP at the beginning, GP at the middle and GP at the end). Each PV array consists of five series-connected modules per string and 54 parallel strings. The I-V & P-V curves of each PV array are shown in Figure 8 and the main characteristic of the module used (CRM185S156P-54 Sunperfect Solar, 3101 N 1st St #107, San Jose, CA, USA) is shown in Table 1.

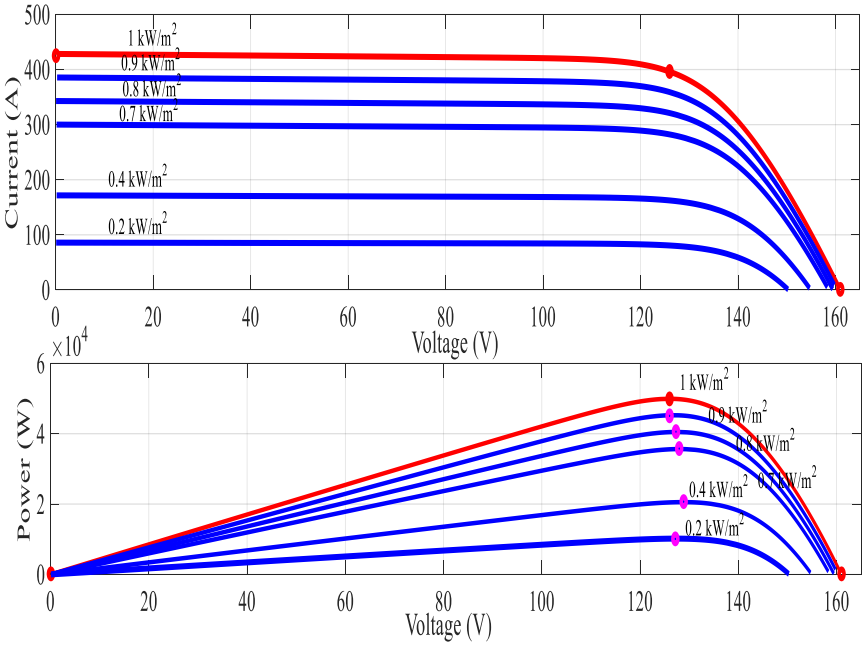


**Figure 8.** I-V and P-V characteristics of the PV array under study.

For comparison purposes, the power circuit and inputs of the two PSPV systems are the same, except for the DC-DC converter. The first PSPV system contains three PSPV arrays is interconnected to the grid through CBC and three-phase inverter as shown previously in Figure 2. DPSO technique is used to track the GP via sending the duty cycle to the CBC, whereas, the second PV system contains the same three PSPV arrays interconnected to the grid through IBC and three-phase inverter as shown previously in Figure 4. A separate P&O MPPT tracker is used to track the peak power for each PV array individually and the total power generated from this system is equal to the summation of all peaks also shown previously in Figure 4. In addition, a fixed IBC (parallel) is used not only to share the currents among inductors but also to regulate and stabilize the DC-link voltage. Hence, IBC performed well compared to CBC in terms of power generated, efficiency, reliability, flexibility, reduction in size and total cost of the generated power. Also, future enlargements of the PV system can be adopted where multi-PV arrays can be added easily as an add-on option with their own boost converter into the existing PV system. Therefore, the incorporation of the IBC instead of CBC under partial shading will attain more technical and economical benefits.

**Table 1.** The electrical characteristics of Sunperfect Solar CRM185S156P-54 module.

| | |
|---|---|
| Maximum power ($P_{\max}$) | 185.22 W |
| Cells per Module | 54 |
| Open-circuit voltage ($V_{oc}$) | 32.2 V |
| Short-circuit current ($I_{sc}$) | 7.89 A |
| Voltage at maximum power point ($V_{MPP}$) | 25.2 V |
| Current at maximum power point ($I_{MPP}$) | 7.35 A |

Different radiation on each PV array generates different power from one PV array to another and multiple peaks will be generated as shown in Table 2. A comparison between the actual power captured with the theoretical one for the three different PS cases is shown in Table 2. The theoretical power is the summation of individual peaks power of the three PV arrays. The actual power generated equals to the GP power in the case of the first PSPV system with CBC, whereas the actual power generated equals to the summation of individual peaks of the three PV arrays in the case of the second PSPV system with IBC which is higher than GP in all cases of PS as shown in Table 2. On the other hand, *MML* is calculated based on Equation (1) for the two PSPV systems for comparison purposes. As the *MML* increases, the actual generated power from the PV system also increases and vice versa. Therefore, improving the *MML* represents a priority to extract high output power generated and improve the power quality. Tracking the GP instead of LPs will improve the *MML*, but does not guarantee the extraction of the maximum power available from the whole PV system. The proposed PV system with IBC works at its MPP and each PV array works at its own MPP, the MML is 100% regardless of whether PS occurred or not as shown in Table 2.

**Table 2.** Mismatch loss comparisons of the three PS different cases with and without IBC.

| **PS Cases** | | **Case 1 (GP at the Beginning)** | | **Case 2 (GP in the Middle)** | | **Case 3 (GP at the End)** | |
|---|---|---|---|---|---|---|---|
| | | $I_r$ **(W/m$^2$)** | ***MP*** **(kW)** | $I_r$ **(W/m$^2$)** | ***MP*** **(kW)** | $I_r$ **(W/m$^2$)** | ***MP*** **(kW)** |
| PV arrays | PV array 1 | 1000 | 50 | 800 | 40.5 | 1000 | 50 |
| | PV array 2 | 400 | 20.6 | 400 | 20.6 | 700 | 35.6 |
| | PV array 3 | 200 | 10.2 | 700 | 35.6 | 900 | 45.3 |
| With CBC | Theoretical Power (kW) | 80.8 | | 96.7 | | 130.9 | |
| | Actual Power (kW) | 50 | | 74 | | 116 | |
| | *MML* | 38.5% | | 40.5% | | 44.8% | |
| With IBC | Theoretical Power (kW) | 80.8 | | 96.7 | | 130.9 | |
| | Actual Power (kW) | 80.8 | | 96.7 | | 130.9 | |
| | *MML* | 100% | | 100% | | 100% | |

Figure 9a shows both the theoretical and actual powers generated from the PV system with CBC, whereas Figure 9b shows both the theoretical and actual powers generated from the PV system with IBC. It is concluded that there is a significant reduction in the actual power generated from the PSPV system with CBC compared to the theoretical power. In contrast, the theoretical and actual powers generated from the PV system with IBC are almost of equal values. Hence, the overall efficiency and the PV system reliability with IBC are improved. Figure 10 shows the actual power generated from the PSPV system with CBC and IBC for the three cases of PS (GP at the beginning, GP at the middle and GP at the end). Fortunately, the actual power generated from the PSPV system with IBC is higher by 61.6%, 30.3% and 13%, respectively, compared to the one generated from PSPV system with CBC for the three PSCs, respectively. This emphasizes that the PSPV system with IBC has high power quality through harvesting high generated power and low power losses under PSCs. This can help and support effectively in overcoming the challenges that face the radial distribution system such as the continuous growth of the load demand and how to supply it through renewable distributed generation.

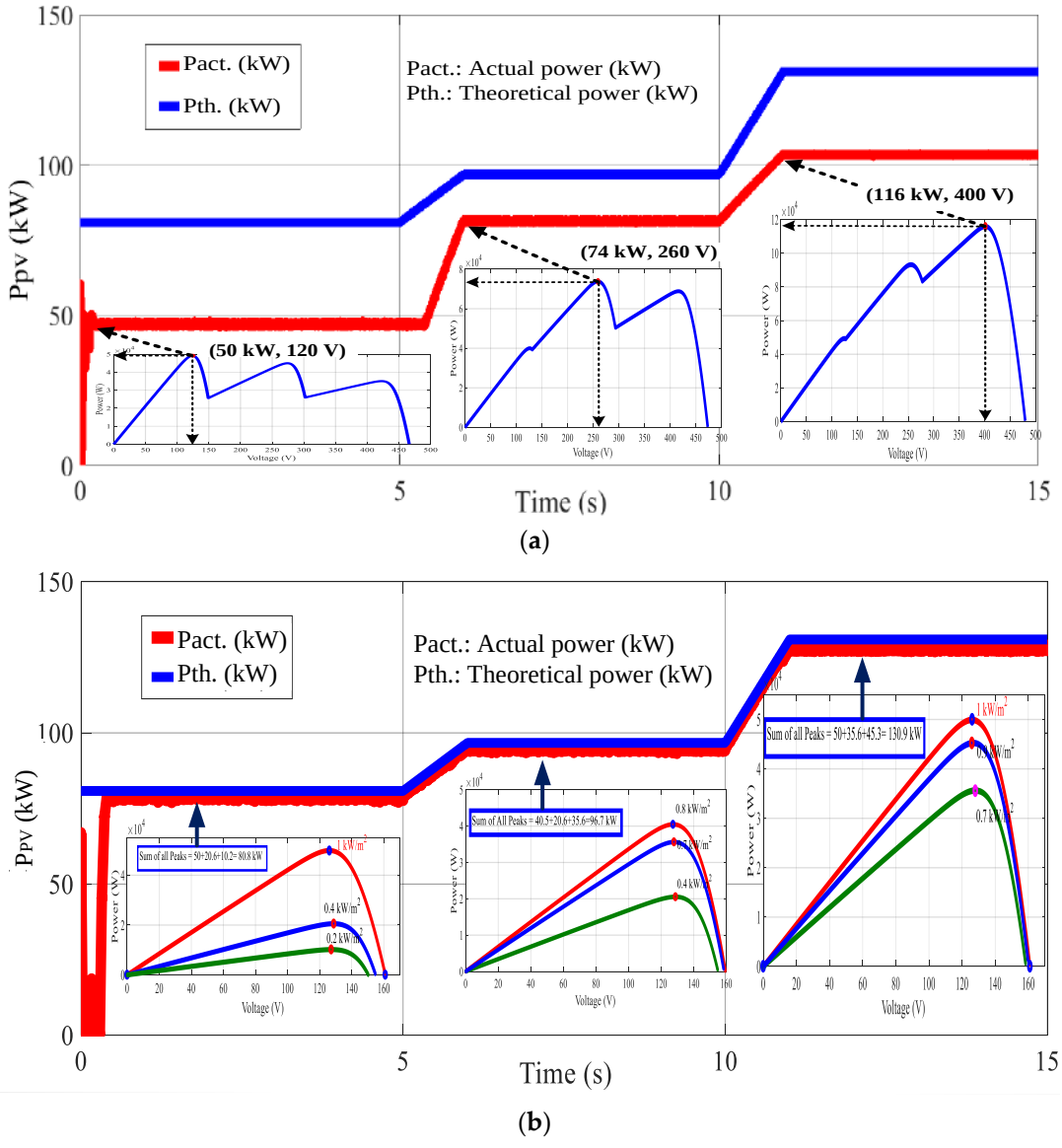


**Figure 9.** The maximum power available from the PSPV: (**a**) With CBC; (**b**) With IBC.

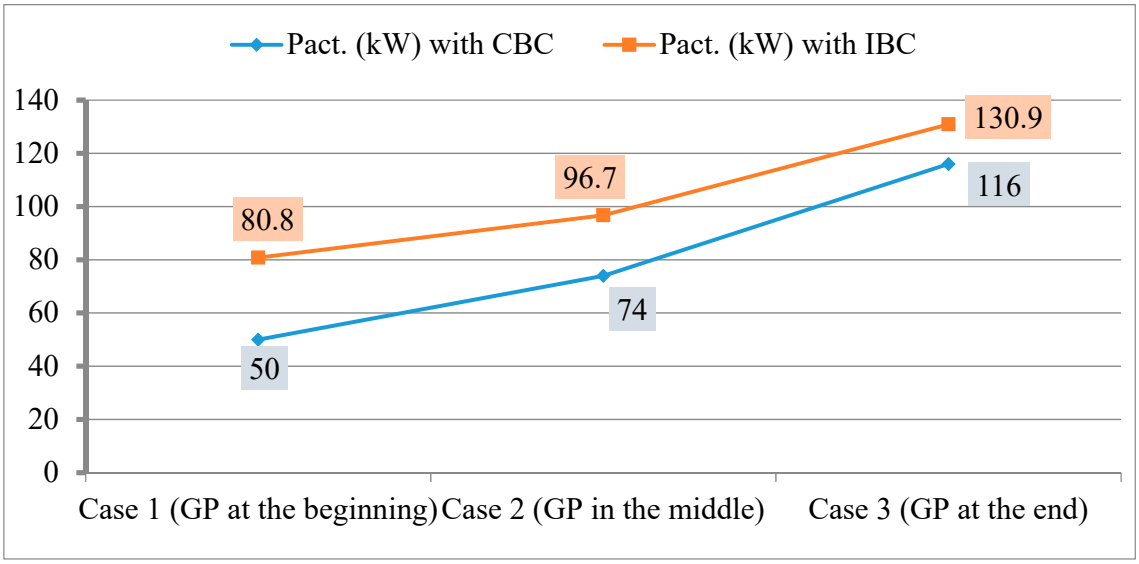


**Figure 10.** The actual power generated from the PSPV system with CBC and IBC for the three cases of PS.

Figure 11 shows the three different duty cycles (*D*1, *D*2 and *D*3) that are sent to the IBC as illustrated previously in Figure 3. Each duty cycle tracks the peak power of its own PV array individually and the total generated power is the summation of all peaks. Figure 12 shows the DC-link voltage (IBC output voltage) which is almost equal to the reference voltage value; 500 V. Hence, fixed IBC enhances the stability and regulation of the DC-link voltage which improves the power quality and stability of the system. The DC-link voltage is regulated and controlled through the three duty cycles while the active and reactive power control are controlled through the modulation index and duty cycles as shown in Figures 12 and 13. Our findings revealed the superiority in performance of multi PSPV with IBC compared to PSPV with CBC in terms of generated power, reliability, DC-link voltage stability and flexibility.

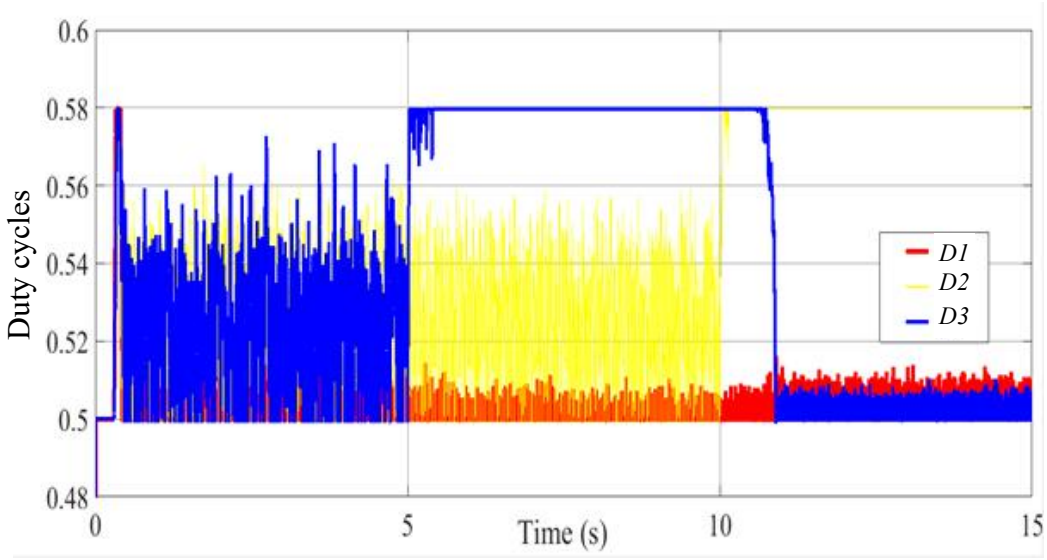


**Figure 11.** The three duty cycles to the IBC.

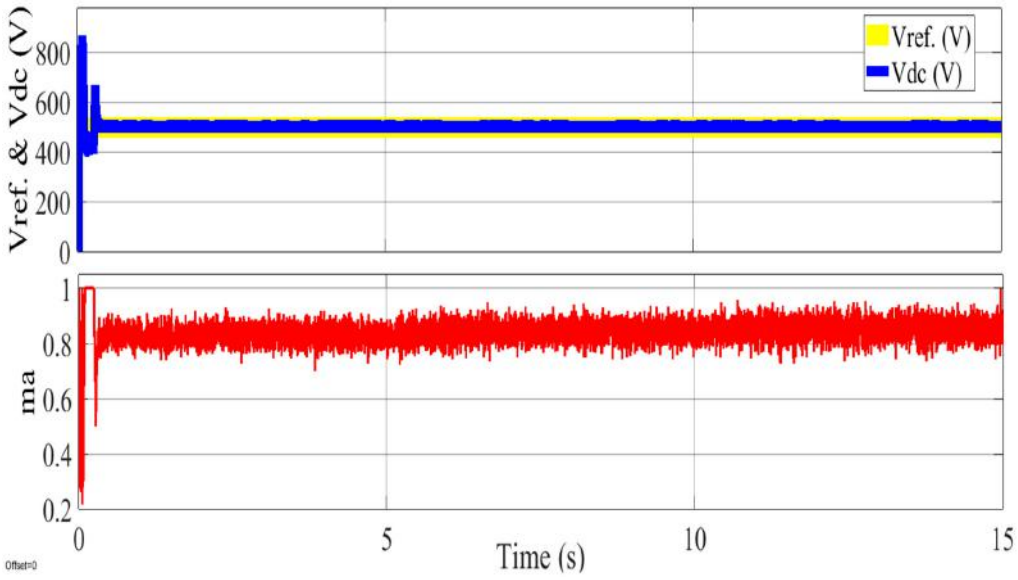


**Figure 12.** The DC-link voltage of the IBC and the modulation index (ma) of the inverter.

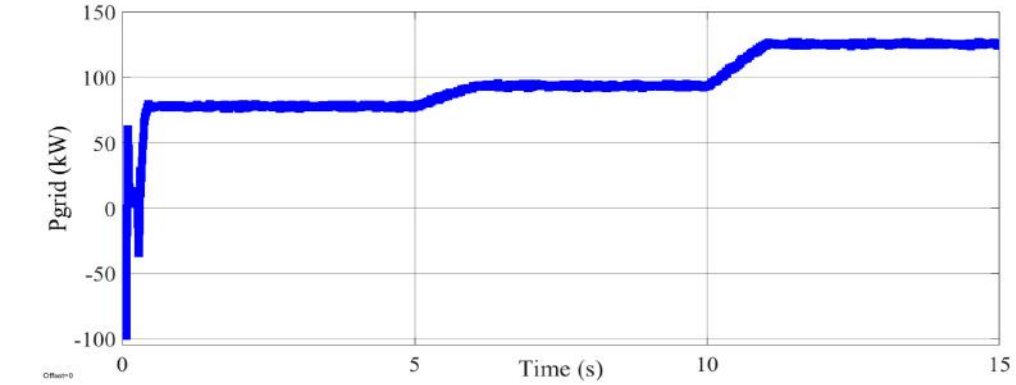


(**a**)

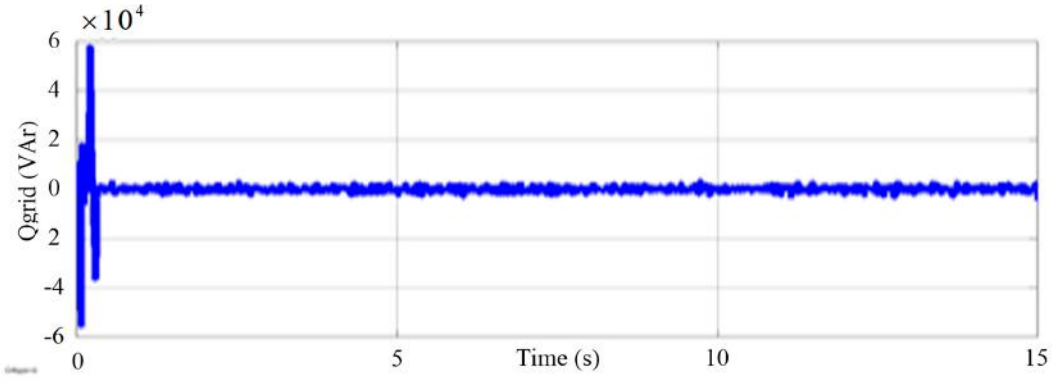


(**b**)

**Figure 13.** The active and reactive power of the utility grid: (**a**) Active power (kW); (**b**) Reactive power (VAr).

## 5. Conclusions

Partial shading (PS) reduces the generated power from PV systems considerably compared to the generation during healthy conditions. Bypass diodes are connected across each PV module to protect the shaded modules or arrays from destruction due to hot-spot effect. In this case, multiple peaks (one GP and many LPs) are generated. Tracking the GP power using efficient soft computing techniques

based on MPPT does not guarantee the extraction of the maximum power available from the PSPV system with CBC. Therefore, the main goal of this study is to propose an effective and efficient solution using IBC, which is not limited to mitigate or alleviate PS effects but also to extract the maximum power available from the whole PSPV system with 100% MML. The second aim of this study is to investigate the performance of IBC interfaced with the PSPV grid-connected compared to the one using CBC. Multi PSPV arrays with IBC using P&O MPP tracker can extract the maximum power available of the whole PV system which is equal to the summation of all peaks of the PV arrays. Whereas, multi PSPV arrays with CBC can extract the GP using DPSO MPP tracker which is lower than the maximum power available from the whole system. The most obvious finding to emerge from this study is that, the power generated from the PSPV system can be increased by 61.6% (Case 1; GP at the beginning), 30.3% (Case 2; GP in the middle) and 13% (Case 3; GP at the end) respectively from the PSPV system by adopting IBC instead of CBC. The results of this investigation have shown that the IBC guarantees the extraction of the maximum power available from the PSPV system with 100% MML, which cannot be attained using CBC. Consequently, an overall efficiency improvement of the presented system was obviously achieved. Furthermore, sharing the input current among the inductors using IBC enhances the PV system's reliability and efficiency. As a result, significant reduction in size and cost is achieved. In addition, power losses can reach 70% of the total generated power with CBC under PSCs, whereas IBC guarantees the extraction of the maximum power available from the PSPV system. Hence, IBC enhances the power quality and reliability of the PSPV system. On the other hand, fixed IBC is similar to the parallel circuit where it enhances the stability of the DC-link voltage. These findings show the superior performance of the proposed PSPV with IBC system compared to the PSPV with CBC in terms of generated power, power quality (less power losses), reliability, efficiency and flexibility.

**Author Contributions:** Conceptualization, H.M.H.F. and A.M.E.; Methodology, H.M.H.F., M.F.O. and A.M.E.; Software, H.M.H.F., A.M.E. and M.F.O.; Validation, H.M.H.F., A.M.E. and M.F.O.; Formal Analysis, H.M.H.F., A.M.E., M.F.O. and M.S.A.-S.; Investigation, H.M.H.F., A.M.E., M.F.O. and M.S.A.-S.; Resources, H.M.H.F., M.F.O. and A.M.E.; Data Curation, H.M.H.F., A.M.E. and M.F.O.; Writing—Original Draft Preparation, H.M.H.F., M.F.O. and A.M.E.; Writing—Review & Editing, H.M.H.F., M.F.O., A.M.E. and M.S.A.-S.; Visualization, H.M.H.F., A.M.E. and M.F.O.; Supervision, M.F.O and A.M.E.; Project Administration, A.M.E.; Funding Acquisition, A.M.E.

**Funding:** The authors extend their appreciation to the Deanship of Scientific Research at King Saud University, Riyadh, Saudi Arabia for funding this work through research group No (RG-1439-66).

**Conflicts of Interest:** The authors declare no conflict of interest.

## Nomenclature

| | |
|---|---|
| $x_i^k$ | Position vector of PSO; |
| $v_i^k$ | Velocity vector of PSO; |
| $\omega$ | Inertia weight; |
| $c_1$ and $c_2$ | The acceleration coefficients; |
| $V_{PV}$ ($i$) | PV voltage for each particle; |
| $I_{PV}$ ($i$) | PV current for each particle; |
| $P_{PV}$ ($i$) | PV output power for each particle; |
| $d_P/d_V$ | Slope of the P-V curve; |
| $I_{MPP}$ | Current at maximum power point; |
| $V_{MPP}$ | Voltage at maximum power point; |
| *MP* | Maximum power generated; |
| *Ir* | irradiance (W/m$^2$); |
| *MML* | Mismatch loss index; |
| PSPV | Partially Shaded Photovoltaic; |
| GP | global peak; |
| LPs | local peaks; |
| MPPT | Maximum Power Point Tracker; |
| IBC | Interleaved Boost Converter; and |
| CBC | Conventional Boost Converter. |

## References


1. Arunkumari, T.; Indragandhi, V. An overview of high voltage conversion ratio DC-DC converter configurations used in DC micro-grid architectures. *Renew. Sustain. Energy Rev.* **2017**, *77*, 670–687. [CrossRef]
2. Babu, T.S.; Rajasekar, N.; Sangeetha, K. Modified particle swarm optimization technique based maximum power point tracking for uniform and under partial shading condition. *Appl. Soft Comput.* **2015**, *34*, 613–624. [CrossRef]
3. Ashouri-Zadeh, A.; Toulabi, M.; Dobakhshari, A.S.; Taghipour-Broujeni, S.; Ranjbar, A.M. A novel technique to extract the maximum power of photovoltaic array in partial shading conditions. *Int. J. Electr. Power Energy Syst.* **2018**, *101*, 500–512. [CrossRef]
4. Saharia, B.J.; Saharia, K.K. Simulated Study on Nonisolated DC-DC Converters for MPP Tracking for Photovoltaic Power Systems. *J. Energy Eng.* **2015**, *142*, 04015001. [CrossRef]
5. Silvestre, S.; Chouder, A. Effects of shadowing on photovoltaic module performance. *Prog. Photovolt. Res. Appl.* **2008**, *16*, 141–149. [CrossRef]
6. Hemandez, J.; Garcia, O.; Jurado, F. Photovoltaic devices under partial shading conditions. *Int. Rev. Model. Simul.* **2012**, *5*, 414–425.
7. Eltamaly, A.M. Performance of smart maximum power point tracker under partial shading conditions of photovoltaic systems. *J. Renew. Sustain. Energy* **2015**, *7*, 043141. [CrossRef]
8. Duong, M.Q.; Sava, G.N.; Ionescu, G.; Necula, H.; Leva, S.; Mussetta, M. Optimal bypass diode configuration for PV arrays under shading influence. In Proceedings of the 2017 IEEE International Conference on Environment and Electrical Engineering and 2017 IEEE Industrial and Commercial Power Systems Europe (EEEIC/I & CPS Europe), Milan, Italy, 6–9 June 2017; pp. 1–5.
9. Rezk, H.; Eltamaly, A.M. A comprehensive comparison of different MPPT techniques for photovoltaic systems. *Sol. Energy* **2015**, *112*, 1–11. [CrossRef]
10. Islam, H.; Mekhilef, S.; Shah, N.B.M.; Soon, T.K.; Seyedmahmousian, M.; Horan, B.; Stojcevski, A. Performance evaluation of maximum power point tracking approaches and photovoltaic systems. *Energies* **2018**, *11*, 365. [CrossRef]
11. Zainuri, M.A.A.M.; Radzi, M.A.M.; Soh, A.C.; Rahim, N.A. Development of adaptive perturb and observe-fuzzy control maximum power point tracking for photovoltaic boost DC–DC converter. *IET Renew. Power Gener.* **2013**, *8*, 183–194. [CrossRef]
12. De Brito, M.A.G.; Galotto, L.; Sampaio, L.P.; Melo, G.d.A.; Canesin, C.A. Evaluation of the main MPPT techniques for photovoltaic applications. *IEEE Trans. Ind. Electron.* **2013**, *60*, 1156–1167. [CrossRef]
13. Ishaque, K.; Salam, Z.; Lauss, G. The performance of perturb and observe and incremental conductance maximum power point tracking method under dynamic weather conditions. *Appl. Energy* **2014**, *119*, 228–236. [CrossRef]
14. Ahmed, J.; Salam, Z. An improved perturb and observe (P&O) maximum power point tracking (MPPT) algorithm for higher efficiency. *Appl. Energy* **2015**, *150*, 97–108.
15. Seyedmahmoudian, M.; Horan, B.; Rahmani, R.; Maung Than Oo, A.; Stojcevski, A. Efficient photovoltaic system maximum power point tracking using a new technique. *Energies* **2016**, *9*, 147. [CrossRef]
16. Teo, J.; Tan, R.H.; Mok, V.; Ramachandaramurthy, V.K.; Tan, C. Impact of Partial Shading on the PV Characteristics and the Maximum Power of a Photovoltaic String. *Energies* **2018**, *11*, 1860. [CrossRef]
17. Ishaque, K.; Salam, Z.; Shamsudin, A.; Amjad, M. A direct control based maximum power point tracking method for photovoltaic system under partial shading conditions using particle swarm optimization algorithm. *Appl. Energy* **2012**, *99*, 414–422. [CrossRef]
18. Bidram, A.; Davoudi, A.; Balog, R.S. Control and circuit techniques to mitigate partial shading effects in photovoltaic arrays. *IEEE J. Photovolt.* **2012**, *2*, 532–546. [CrossRef]
19. Balasubramanian, I.R.; Ganesan, S.I.; Chilakapati, N. Impact of partial shading on the output power of PV systems under partial shading conditions. *IET Power Electron.* **2013**, *7*, 657–666. [CrossRef]
20. Ali, A.I.M.; Sayed, M.A.; Mohamed, E.E.M. Modified efficient perturb and observe maximum power point tracking technique for grid-tied PV system. *Int. J. Electr. Power Energy Syst.* **2018**, *99*, 192–202. [CrossRef]
21. Ji, Y.-H.; Jung, D.-Y.; Kim, J.-G.; Kim, J.-H.; Lee, T.-W.; Won, C.-Y. A real maximum power point tracking method for mismatching compensation in PV array under partially shaded conditions. *IEEE Trans. Power Electron.* **2011**, *26*, 1001–1009. [CrossRef]

22. Titri, S.; Larbes, C.; Toumi, K.Y.; Benatchba, K. A new MPPT controller based on the Ant colony optimization algorithm for Photovoltaic systems under partial shading conditions. *Appl. Soft Comput.* **2017**, *58*, 465–479. [CrossRef]
23. Ishaque, K.; Salam, Z.; Amjad, M.; Mekhilef, S. An improved particle swarm optimization (PSO)–based MPPT for PV with reduced steady-state oscillation. *IEEE Trans. Power Electron.* **2012**, *27*, 3627–3638. [CrossRef]
24. Ishaque, K.; Salam, Z. A review of maximum power point tracking techniques of PV system for uniform insolation and partial shading condition. *Renew. Sustain. Energy Rev.* **2013**, *19*, 475–488. [CrossRef]
25. Ishaque, K.; Salam, Z. A deterministic particle swarm optimization maximum power point tracker for photovoltaic system under partial shading condition. *IEEE Trans. Ind. Electron.* **2013**, *60*, 3195–3206. [CrossRef]
26. Khare, A.; Rangnekar, S. A review of particle swarm optimization and its applications in solar photovoltaic system. *Appl. Soft Comput.* **2013**, *13*, 2997–3006. [CrossRef]
27. Miyatake, M.; Toriumi, F.; Endo, T.; Fujii, N. A Novel maximum power point tracker controlling several converters connected to photovoltaic arrays with particle swarm optimization technique. In Proceedings of the 2007 European conference on Power Electronics and Applications, Aalborg, Denmark, 2–5 September 2007; pp. 1–10.
28. Ishaque, K.; Salam, Z.; Taheri, H.; Shamsudin, A. Maximum power point tracking for PV system under partial shading condition via particle swarm optimization. In Proceedings of the 2011 IEEE Applied Power Electronics Colloquium (IAPEC), Johor Bahru, Malaysia, 18–19 April 2011; pp. 5–9.
29. Sarvi, M.; Ahmadi, S.; Abdi, S. A PSO-based maximum power point tracking for photovoltaic systems under environmental and partially shaded conditions. *Prog. Photovolt. Res. Appl.* **2015**, *23*, 201–214. [CrossRef]
30. Chekired, F.; Mellit, A.; Kalogirou, S.; Larbes, C. Intelligent maximum power point trackers for photovoltaic applications using FPGA chip: A comparative study. *Sol. Energy* **2014**, *101*, 83–99. [CrossRef]
31. Kamarzaman, N.A.; Tan, C.W. A comprehensive review of maximum power point tracking algorithms for photovoltaic systems. *Renew. Sustain. Energy Rev.* **2014**, *37*, 585–598. [CrossRef]
32. Messai, A.; Mellit, A.; Guessoum, A.; Kalogirou, S. Maximum power point tracking using a GA optimized fuzzy logic controller and its FPGA implementation. *Sol. Energy* **2011**, *85*, 265–277. [CrossRef]
33. Eltamaly, A.M. Modeling of fuzzy logic controller for photovoltaic maximum power point tracker. In Proceedings of the Solar Future 2010 Conference, Istanbul, Turkey, 12 February 2010.
34. Chang, L.-Y.; Chao, K.-H.; Chang, T.-C. A High Voltage Ratio and Low Ripple Interleaved DC-DC Converter for Fuel Cell Applications. *Sci. World J.* **2012**, *2012*, 896508. [CrossRef] [PubMed]
35. De Assis Sobreira, P., Jr.; Tofoli, F.L.; Braga, H.A.C.; Barbosa, P.G.; Ferreira, A.A. Analysis of mppt techniques applied to the dcm multiphase boost converter for the mitigation of partial shading in PV arrays. *Eletrôn. Potên.* **2013**, *18*, 1138–1148. [CrossRef]
36. Coruh, N.; Urgun, S.; Erfidan, T.; Ozturk, S. A simple and efficient implemantation of interleaved boost converter. In Proceedings of the 2011 6th IEEE Conference on Industrial Electronics and Applications (ICIEA), Beijing, China, 21–23 June 2011; pp. 2364–2368.
37. Lee, P.-W.; Lee, Y.-S.; Cheng, D.K.; Liu, X.-C. Steady-state analysis of an interleaved boost converter with coupled inductors. *IEEE Trans. Ind. Electron.* **2000**, *47*, 787–795. [CrossRef]
38. Liccardo, F.; Marino, P.; Torre, G.; Triggianese, M. Interleaved dc-dc converters for photovoltaic modules. In Proceedings of the 2007 ICCEP'07, International Conference on Clean Electrical Power, Capri, Itlay, 21–23 May 2007; pp. 201–207.
39. Sri Revathi, B.; Prabhakar, M. Non isolated high gain DC-DC converter topologies for PV applications—A comprehensive review. *Renew. Sustain. Energy Rev.* **2016**, *66*, 920–933. [CrossRef]
40. Garth, D.R.; Muldoon, W.; Benson, G.; Costague, E. Multi-phase, 2-kilowatt, high-voltage, regulated power supply. In Proceedings of the 1971 IEEE Power Electronics Specialists Conference, Pasadena, CA, USA, 19–20 April 1971; pp. 110–116.
41. Benyahia, N.; Denoun, H.; Badji, A.; Zaouia, M.; Rekioua, T.; Benamrouche, N.; Rekioua, D. MPPT controller for an interleaved boost dc–dc converter used in fuel cell electric vehicles. *Int. J. Hydrogen Energy* **2014**, *39*, 15196–15205. [CrossRef]

42. Arango, E.; Ramos-Paja, C.A.; Calvente, J.; Giral, R.; Serna, S. Asymmetrical interleaved DC/DC switching converters for photovoltaic and fuel cell applications—Part 1: Circuit generation, analysis and design. *Energies* **2012**, *5*, 4590–4623. [CrossRef]
43. Deihimi, A.; Mahmoodieh, M.E.S.; Iravani, R. A new multi-input step-up DC–DC converter for hybrid energy systems. *Electr. Power Syst. Res.* **2017**, *149*, 111–124. [CrossRef]
44. Mohapatra, A.; Nayak, B.; Das, P.; Mohanty, K.B. A review on MPPT techniques of PV system under partial shading condition. *Renew. Sustain. Energy Rev.* **2017**, *80*, 854–867. [CrossRef]
45. Lakpathi, G.; Reddy, S.M.; Ganesh, K.L.; Satyanarayana, G. An effective high step-up interleaved DC-DC converter photovoltaic grid connection System. *Int. J. Soft Comput. Eng. (IJSCE)* **2013**, *3*, 2231–2307.
46. Khadmun, W.; Subsingha, W. High Voltage Gain Interleaved DC Boost Converter Application for Photovoltaic Generation System. *Energy Procedia* **2013**, *34*, 390–398. [CrossRef]
47. Khosroshahi, A.; Abapour, M.; Sabahi, M. Reliability evaluation of conventional and interleaved DC–DC boost converters. *IEEE Trans. Power Electron.* **2015**, *30*, 5821–5828. [CrossRef]
48. Henn, G.A.; Silva, R.; Praca, P.P.; Barreto, L.H.; Oliveira, D.S. Interleaved-boost converter with high voltage gain. *IEEE Trans. Power Electron.* **2010**, *25*, 2753–2761. [CrossRef]
49. Yang, B.; Li, W.; Zhao, Y.; He, X. Design and analysis of a grid-connected photovoltaic power system. *IEEE Trans. Power Electron.* **2010**, *25*, 992–1000. [CrossRef]
50. Ramaprabha, R.; Balaji, K.; Raj, S.; Logeshwaran, V. Comparison of interleaved boost converter configurations for solar photovoltaic system interface. *J. Eng. Res. [TJER]* **2013**, *10*, 87–98. [CrossRef]
51. Prasanth, P.; Seyezhai, R. Investigation of four phase interleaved boost converter under open loop and closed loop control schemes for battery charging applications. *Int. J. Adv. Materi. Sci. Eng. (IJAMSE)* **2016**, *5*, 2201–2311. [CrossRef]
52. Aghdam, F.H.; Hagh, M.T.; Abapour, M. Reliability evaluation of two-stage interleaved boost converter interfacing PV panels based on mode of use. In Proceedings of the 2016 7th Power Electronics and Drive Systems Technologies Conference (PEDSTC), Tehran, Iran, 16–18 February 2016; pp. 409–414.
53. Lai, C.-M.; Cheng, Y.-H.; Teh, J.; Lin, Y.-C. A New Combined Boost Converter with Improved Voltage Gain as a Battery-Powered Front-End Interface for Automotive Audio Amplifiers. *Energies* **2017**, *10*, 1128. [CrossRef]
54. Rehman, Z.; Al-Bahadly, I.; Mukhopadhyay, S. Multiinput DC–DC converters in renewable energy applications—An overview. *Renew. Sustain. Energy Rev.* **2015**, *41*, 521–539. [CrossRef]
55. Ho, C.N.-M.; Breuninger, H.; Pettersson, S.; Escobar, G.; Canales, F. A comparative performance study of an interleaved boost converter using commercial Si and SiC diodes for PV applications. *IEEE Trans. Power Electron.* **2013**, *28*, 289–299. [CrossRef]
56. Mouli, G.R.C.; Schijffelen, J.H.; Bauer, P.; Zeman, M. Design and Comparison of a 10-kW Interleaved Boost Converter for PV Application Using Si and SiC Devices. *IEEE J. Emerg. Sel. Top. Power Electron.* **2017**, *5*, 610–623. [CrossRef]
57. Eltamaly, A.M.; Alolah, A.; Farh, H.M. Maximum power extraction from utility-interfaced wind turbines. In *New Developments in Renewable Energy*; InTech: London, UK, 2013.
58. Al-Obeidat, F.; Belacel, N.; Carretero, J.A.; Mahanti, P. Automatic Parameter Settings for the PROAFTN Classifier Using Hybrid Particle Swarm Optimization. In Proceedings of the Canadian Conference on AI, Ottawa, ON, Canada, 31 May–2 June 2010; pp. 184–195.
59. Liu, Y.; Xia, D.; He, Z. MPPT of a PV system based on the particle swarm optimization. In Proceedings of the 2011 4th International Conference on Electric Utility Deregulation and Restructuring and Power Technologies (DRPT), Weihai, China, 6–9 July 2011; pp. 1094–1096.
60. Miyatake, M.; Inada, T.; Hiratsuka, I.; Zhao, H.; Otsuka, H.; Nakano, M. Control characteristics of a fibonacci-search-based maximum power point tracker when a photovoltaic array is partially shaded. In Proceedings of the IPEMC 2004, the 4th International Power Electronics and Motion Control Conference, Xi'an, China, 14–16 August 2004; pp. 816–821.
61. Soltani, I.; Sarvi, M.; Marefatjou, H. An intelligent, fast and robust maximum power point tracking for proton exchange membrane fuel cell. *World Appl. Program.* **2013**, *3*, 264–281.
62. Huang, Y.-P.; Ye, C.-E.; Chen, X. A Modified Firefly Algorithm with Rapid Response Maximum Power Point Tracking for Photovoltaic Systems under Partial Shading Conditions. *Energies* **2018**, *11*, 2284. [CrossRef]

63. Ahmed, J.; Salam, Z. A Maximum Power Point Tracking (MPPT) for PV system using Cuckoo Search with partial shading capability. *Appl. Energy* **2014**, *119*, 118–130. [CrossRef]
64. Chang, L.-Y.; Chung, Y.-N.; Chao, K.-H.; Kao, J.-J. Smart Global Maximum Power Point Tracking Controller of Photovoltaic Module Arrays. *Energies* **2018**, *11*, 567. [CrossRef]
65. Khadidja, S.; Mountassar, M.; M'hamed, B. Comparative study of incremental conductance and perturb & observe MPPT methods for photovoltaic system. In Proceedings of the 2017 International Conference on Green Energy Conversion Systems (GECS), Hammamet, Tunisia, 23–25 March 2017; pp. 1–6.
66. Sharma, R.S.; Katti, P. Perturb & observation MPPT algorithm for solar photovoltaic system. In Proceedings of the 2017 International Conference on Circuit, Power and Computing Technologies (ICCPCT), Kollam, India, 20–21 April 2017; pp. 1–6.